Available online at www.sciencedirect.com
SCIENCE DIRECT®
Astroparticle Physics 21 (2004) 597–607
Astroparticle Physics
www.elsevier.com/locate/astropart

The mass composition of cosmic rays near 10^{18} eV as deduced from measurements made at Volcano Ranch

M.T. Dova [a], M.E. Manceñido [a], A.G. Mariazzi [a], T.P. McCauley [b], A.A. Watson [c,*]

[a] *Instituto de Física, CONICET, Dto. de Física, Universidad Nacional de La Plata, C.C.67, 1900 La Plata, Argentina*
[b] *Department of Physics, Northeastern University, Boston, MA 02115, USA*
[c] *School of Physics and Astronomy, University of Leeds, Leeds LS2 9JT, UK*

Received 4 September 2003; received in revised form 7 April 2004; accepted 16 April 2004
Available online 8 June 2004

Abstract

Linsley used the Volcano Ranch array to collect data on the lateral distribution of showers produced by cosmic rays at energies above 10^{17} eV. Very precise measurements of the steepness of the lateral distribution function were made on 366 events. The current availability of sophisticated hadronic interaction models has prompted an interpretation of the measurements. In this analysis we use the AIRES Monte Carlo code to generate showers, together with GEANT4 to simulate the detector response to ground particles. The results show that, with the assumption of a bi-modal proton and iron mix, iron is the dominant component of cosmic rays near 10^{18} eV, assuming that hadronic interactions are well-described by QGSJET at this energy range. The Volcano Ranch data set, as available to us, does not allow a straightforward assignment of energy for each event. It is thus not possible to give the energy dependence of the mass composition.

PACS: 96.40.−z; 13.85.Tn

1. Introduction

The measurement of the mass composition of cosmic rays above 10^{17} eV is a challenging problem. This information is as important as the energy spectrum and the anisotropy in determining cosmic ray origin. For example, one must know the likely mass range of a particular data set before one can interpret anisotropy information confidently, given the influence of galactic and intergalactic magnetic fields. Our knowledge of the mass composition of cosmic rays above 10^{17} eV remains very limited. Recent re-interpretation of measurements of the lateral distribution of water-Čerenkov signals made at Haverah Park [1] suggests a composition of 34% protons and 66% iron in the range 2×10^{17}–10^{18} eV. This contrasts with earlier claims, from observations made using Fly's Eye, that the composition changes from a heavy mix around 3×10^{17} eV to a proton dominated flux

* Corresponding author.
E-mail address: a.a.watson@leeds.ac.uk (A.A. Watson).

0927-6505/$ - see front matter © 2004 Elsevier B.V. All rights reserved.
doi:10.1016/j.astropartphys.2004.04.009

around 10^{19} eV [2,3]. At Yakutsk, both the inferred values of the depth of shower maximum (X_{max}) and the muon density favor a composition change from a mixture of heavy and light components to light composition over the same energy region [9]. From HiRes/MIA data [7], there are claims that there is a rapid change from a heavy to a light composition between 0.1 and 1.0 EeV. A recent analysis by the HiRes collaboration of data collected in the energy range between 10^{18} and $10^{19.4}$ eV [8] is consistent with a nearly constant, purely protonic composition. The fraction of protons however, decreases when they interpret their data using the hadronic interaction generator SIBYLL2.1 in their analysis. On the other hand, the AGASA group have argued for a "mixed" unchanging composition from 1 to 10 EeV [4] (using MOCCA for the simulations). A recent analysis of the muon component in air showers with AIRES/QGSJET98 around 10^{19} eV by the AGASA collaboration indicates a relatively light average composition [5].

The source of the discrepancies between different experiments is not understood and it is important to resolve the issue because of its implications for cosmic ray models of origin, acceleration and propagation. Volcano Ranch data may provide a path for further understanding. Following the successful re-examination of the Haverah Park data [1] with modern shower models, we report here a similar analysis using the Volcano Ranch data, collected by Linsley et al. [16] to determine the shape of the lateral distribution of air showers. However, the Volcano Ranch data set, as it is available to us, does not allow an energy assignment to be made to individual events. It is thus not possible to give the energy dependence of the mass composition. This is the first attempt to examine the Volcano Ranch data with the results of Monte Carlo calculations, using Monte Carlo tools that were unavailable when the data were recorded in 1970s. It is timely as the situation on mass composition above 10^{17} eV remains confused: the steepness of the lateral distribution is sensitive to the depth of maximum of the shower, and therefore to the primary composition and to the character of the initial hadronic interactions.

To simulate the development of the air showers, we have used the AIRES [10] code (version 2.4.0), with the hadronic interaction generator QGSJET98 [11]. The results of the simulated showers were convolved with a simulation of the detector response made using GEANT4 [15]. A comparison of two hadronic generators (QGSJET98 and SIBYLL2.1 [12]) was presented in [26]. Both give satisfactory descriptions of the Volcano Ranch data, but we have preferred to use QGSJET98 because this model has been shown to be consistent with experimental data at energies up to 10 PeV and beyond [13,14].

Three different kind of "smoothings" have been performed on the Monte Carlo data to make them consistent with the experimental records. The first one is unavoidable and characteristic of any analysis of this type, and is due to the thinning procedure used in Monte Carlo shower propagation codes. Thus, to simulate the response of the detectors correctly, it is necessary to perform a smoothing of the densities of the ground particles at the position of each detector. This is equivalent to sampling particles on a larger area to get a realistic density at the detector position. The second was performed to include, within the simulation, the effect of data reconstruction. We smeared each value of η (the steepness of the lateral distribution) calculated by Monte Carlo using a Gaussian with a width chosen so that Linsley's overall uncertainties in η are reproduced. We find that the width is much smaller than the shower-to-shower fluctuations. The third smoothing relates to the energy range and is discussed in Section 5.1.

2. The Volcano Ranch array

The pioneering Volcano Ranch instrument consisted of an array of scintillation counters. The array was operated in three configurations from 1959 to 1976 at the MIT Volcano Ranch station located near Albuquerque, New Mexico (at an atmospheric depth of 834 $g\,cm^{-2}$). One of its many distinctions was the detection of the first cosmic ray with an energy estimated at 10^{20} eV [19]. The final configuration, of relevance here, comprised 80 detectors of surface area 0.815 m^2 and thickness 9.032 $g\,cm^{-2}$, laid out on a hexagonal grid with a

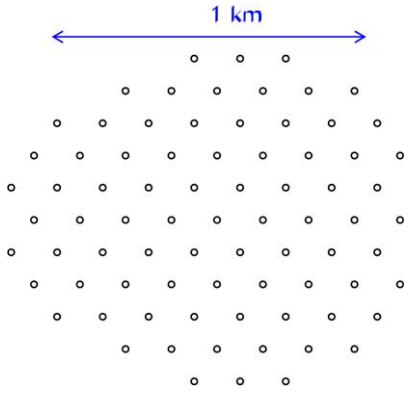

Fig. 1. Volcano Ranch array in the final configuration.

separation of 147 m (Fig. 1). This configuration allowed precise measurement of the lateral distribution of the detector signals. The steepness of the lateral distribution, and its fluctuations, can be used to explore the primary mass composition as in [1]. Fortunately, in his various writings, Linsley has left unusually detailed descriptions of his equipment, together with examples of events and a description of his data reduction methods.

3. Lateral distribution function

A generalized version of the Nishimura–Kamata–Greisen (NKG) formula was used to describe the lateral distribution of particles at ground in minimum ionizing particles per square metre (mips m^{-2}) for Volcano Ranch data [24]. This lateral distribution function is given as

$$S_{\mathrm{VR}}(r) = \frac{N}{r_{\mathrm{m}}^2} C(\alpha,\eta)\left(\frac{r}{r_{\mathrm{m}}}\right)^{-\alpha}\left(1+\frac{r}{r_{\mathrm{m}}}\right)^{-(\eta-\alpha)} \quad (1)$$

normalized to shower size N with

$$C = \frac{\Gamma(\eta-\alpha)}{2\pi\Gamma(2-\alpha)\Gamma(\eta-2)}. \quad (2)$$

Here r_{m} is the Molière radius, which is $\simeq$100 m for the Volcano Ranch elevation. η and α are parameters that describe the logarithmic slope of this function.

From a subset of 366 showers detected with the array, the form of η as a function of zenith angle θ and shower size N was found to be [20]:

$$\langle \eta(\theta,N)\rangle = a + b(\sec\theta - 1) + c\log_{10}\left(\frac{N}{10^8}\right) \quad (3)$$

with $a = 3.88 \pm 0.054$, $b = -0.64 \pm 0.07$, and $c = 0.07 \pm 0.03$ where a fixed value of $\alpha = 1$ was adopted.

4. Simulation of the detector response of the Volcano Ranch array

The AIRES code provides a realistic air shower simulation system, which includes electromagnetic algorithms [18] and links to different hadronic interaction models. As mentioned above, we have used the QGSJET98 model for nuclear fragmentation and inelastic collisions. For the highest energy showers, the number of secondaries becomes so large that it is prohibitive in computing time and disk space to follow and store all of them. Hillas [17] introduced a non-uniform statistical sampling mechanism which allows reconstruction of the whole extensive air shower from a small but representative fraction of secondaries that are fully tracked. Statistical weights are assigned to the sampled particles to account for the energy of the discarded particles. This technique is known as "statistical thinning". The AIRES code includes an extended thinning algorithm, which has been explained in detail [10]. The present work has been carried out using, in most cases, an effective thinning level $\epsilon_{\mathrm{th}} = E_{\mathrm{th}}/E_{\mathrm{prim}} = 10^{-7}$ which is sufficient to avoid the generation of spurious fluctuations and to provide a statistically reliable sample of particles far from the shower core. All shower particles with energies above the following thresholds were tracked: 90 keV for photons, 90 keV for electrons and positrons, 10 MeV for muons, 60 MeV for mesons and 120 MeV for nucleons and nuclei.

We have generated a total of 1735 proton and iron showers with zenith angles in the range $\sec\theta = 1.0$–1.5 and primary energies between 10^{17} and 10^{19} eV to match the Volcano Ranch data. To simulate the response of the detectors of the array to the ground particles, we utilized the general-purpose simulation toolkit GEANT4. Our procedure follows the prescription in [23], where the

detector response to electrons, gamma, and muons is simulated in the energy range 0.1–10^5 MeV and for five bins per decade of energy. The results of air shower simulations are convolved with the detector response to obtain the scintillator yield expressed in mips m^{-2}. The computed lateral distributions of particles and the corresponding signal from the scintillators for photons, electrons and muons are displayed in Fig. 2.

A comparison between the lateral distribution measurements [24] and proton/iron showers simulated with AIRES/QGSJET98 including the scintillator response was presented previously [26]. Each simulated shower was thrown a maximum of 100 times on to the simulated Volcano Ranch array with random core positions in the range 0–500 m from the array center.

With the thinning method used in Monte Carlo shower propagation codes, when particles reach the thinning energy just one of them is followed and is multiplied by a corresponding weight at the end. Thus, to simulate the response of the detectors correctly, it is necessary to perform a smoothing of the densities of the ground particles around the position of each detector. All particles in a "sampling zone" around a given detector are selected and the statistical weight, as obtained from AIRES, is multiplied by the "sampling ratio" $A_{\text{detector}}/A_{\text{sampling}}$, where A_{sampling} is the area of the "sampling zone" and A_{detector} is the corresponding detector area. This is equivalent to sampling particles on a larger area to get a realistic density around the detector position. As the densities depend mainly on the distance to the shower axis, the sampling area over which simulated particles are gathered is such that this ratio varies from about 0.1 at 100 m to about 0.001 at 1 km. As a first check on the validity of our approach, the data of a single large event were compared with calculations [26]. Further checks between data and Monte Carlo calculations were performed such as the one shown in Fig. 3. In this plot we present a comparison between lateral distribution measurements [24] and a $10^{19.1}$ eV proton (left) and iron (right) shower simulated with AIRES/QGSJET98, including the scintillator response of the detectors in the Volcano Ranch array configuration. It has been shown that the fluctuation of the density of shower particles far from the core is quite small and that the density at 600 m, $S(600)$, depends only on primary energy [25]. We normalize the showers to the value of $S(600)$ to decouple the normalization factor from the parameters related to the shape of the lateral distribution which change with primary mass. The agreement between data and Monte Carlo is good and gives confidence in the procedures used.

5. Derivation of the primary mass composition

The nature of the primaries that initiate air showers is difficult to establish from the average properties of the data. For example, an average property can be explained with a mass composition of a single species (A) or by an appropriate

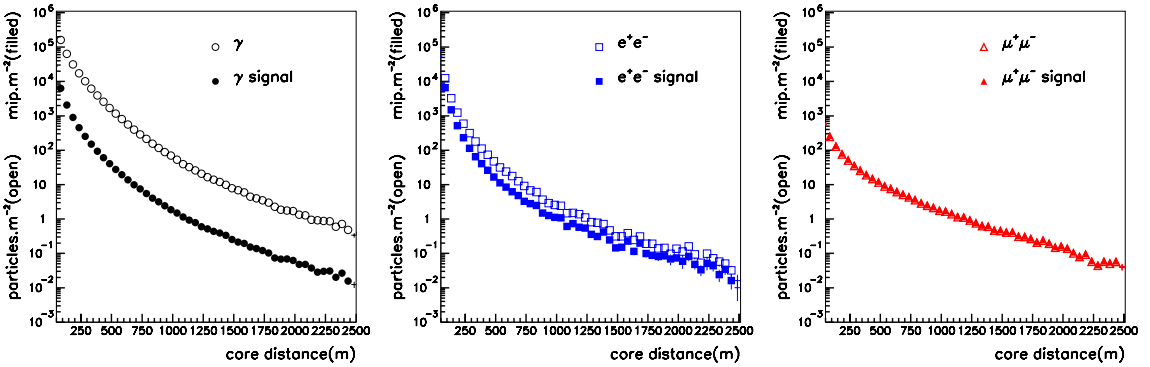

Fig. 2. Simulated lateral distributions of the three main shower components at ground level and its convolution with the detector response (the signal).

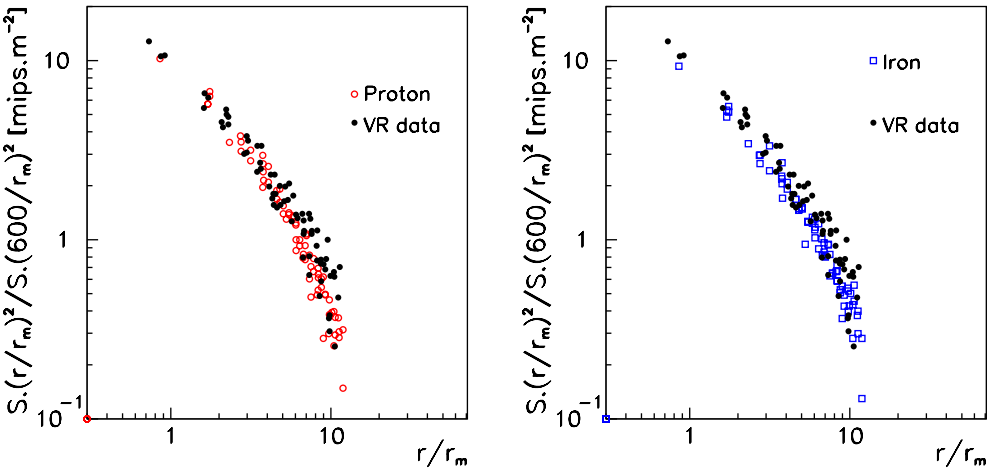

Fig. 3. Comparison between lateral distribution measurements in a single event [24] and the simulated scintillator response in the configuration of VR array for $10^{19.1}$ eV proton and iron showers.

mixture of species. However, with the Volcano Ranch array, accurate measurements of η were made on a shower-by-shower basis for fixed bins of zenith angle separated by 80 g cm^{-2} [21]. Thus the fluctuations of η can be used to break this degeneracy [22]. Linsley determined the precision of each measurement of η and reported the average value of this quantity for each zenith angle bin.

The average error in η from the fit made to the simulated lateral distributions ($\sigma_{\text{sim}} = 0.029$), is smaller than the one reported by Linsley ($\sigma = 0.072$). To include within the simulation the effect of data reconstruction, we smeared each value of η calculated by Monte Carlo using a Gaussian with a width chosen so that Linsley's overall uncertainties in η are reproduced. This width, $\sigma_{\text{smear}} = 0.066$, is found by quadratic subtraction of the average values of σ_{sim} and σ. This is a minor correction, since the measurement precision is much smaller than the size of the intrinsic shower-to-shower spread (r.m.s. = 0.19). Thus, for each value of η found from the Monte Carlo calculations, we have a corresponding and realistic estimate of its "experimental" uncertainty. We are thus able to make comparisons of Volcano Ranch data with our calculations.

As a further check, we have calculated the variation of η with shower size and zenith angle with Monte Carlo and made comparisons with the Volcano Ranch data. The number of particles at ground level (N_{fit}) is obtained from a fit to the lateral distribution function (with $\alpha = 1$) for fixed bins of zenith angle. The variation of η with N_{fit} from the calculation has been compared with the average functional form of η given by Eq. (3). The results of this comparison for $\sec\theta = 1.0$–1.1 and 1.3–1.4 can be seen for proton and iron showers in Fig. 4. The error bars indicate the r.m.s. spreads of data which are very much greater than the r.m.s. spreads of the mean. The shaded band represents the fit to Volcano Ranch data, including the errors given for a and b in Eq. (3).

The variation of η with zenith angle is shown in Fig. 5 for events with shower size in the range $\log N_{\text{fit}} = 7.6$–$8.6$ (left) and $\log N_{\text{fit}} = 8.6$–$9.6$ (right). One can see that the average form of η over a realistic range of mass composition, from proton to iron, is well-represented by the simulations. The error bars represent the r.m.s. spreads as before.

5.1. Fitting VR data mass composition using finite Monte Carlo samples of different primaries

We can estimate the primary mass that describes the Volcano Ranch data, assuming a bimodal composition, using a maximum likelihood fit for the best linear combination of pure iron and pure proton samples to match the data

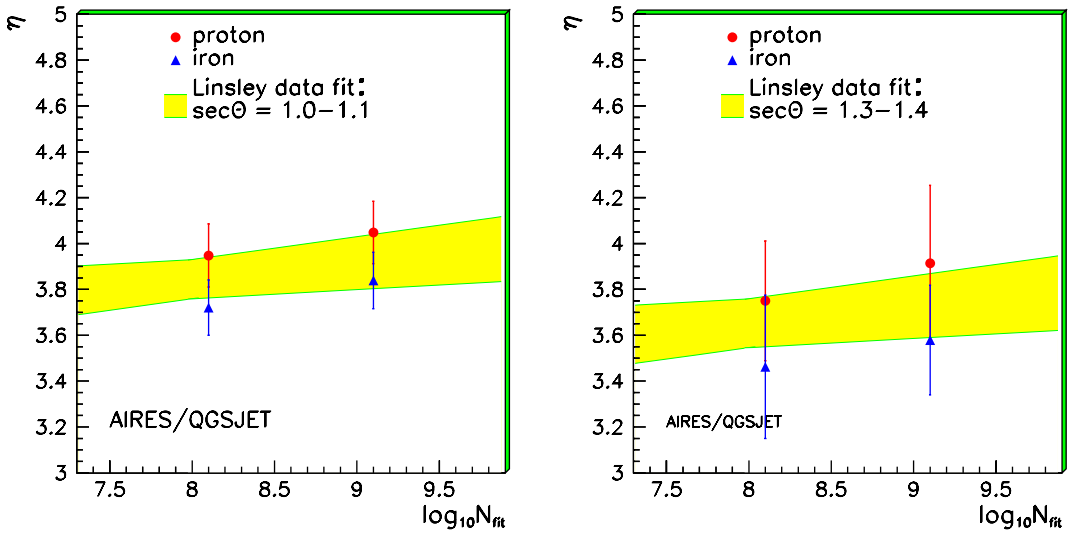

Fig. 4. Comparison of η as a function of shower size for $\sec\theta = 1.0$–1.1 (left) and $\sec\theta = 1.3$–1.4 (right) using AIRES/QGSJET98.

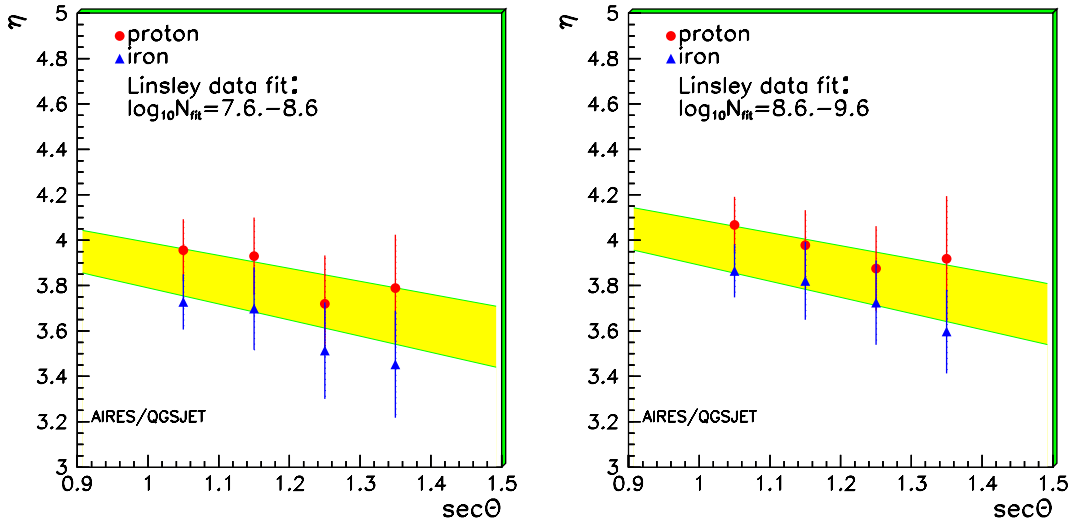

Fig. 5. Comparison of η as a function of $\sec\theta$ for the first bin (left) and second bin (right) in $\log N_{\text{fit}}$.

sample. The available data are in bins of η [21]; the number of data points in several bins is small, so a χ^2 minimization is inappropriate. A maximum likelihood technique assuming Poisson statistics was adopted. The probability of observing a particular number of events d_i in a particular bin is given by $\exp(-f_i)f_i^{d_i}/d_i!$, where f_i is the predicted value for the number of events in this particular bin. If we assume a bi-modal composition of proton and iron with fractions P_{Fe} and P_{p} then $f_i = C(P_{\text{Fe}} + P_{\text{p}})$, where C is the overall normalization factor between numbers of data and Monte Carlo events. Estimates of the fractions P_j are found by maximizing $\ln(L) = \sum d_i \ln(f_i) - \ln(d_i!) - f_i$. Our Monte Carlo samples are at least 10 times larger than the data sample to avoid effects of finite Monte Carlo data size.

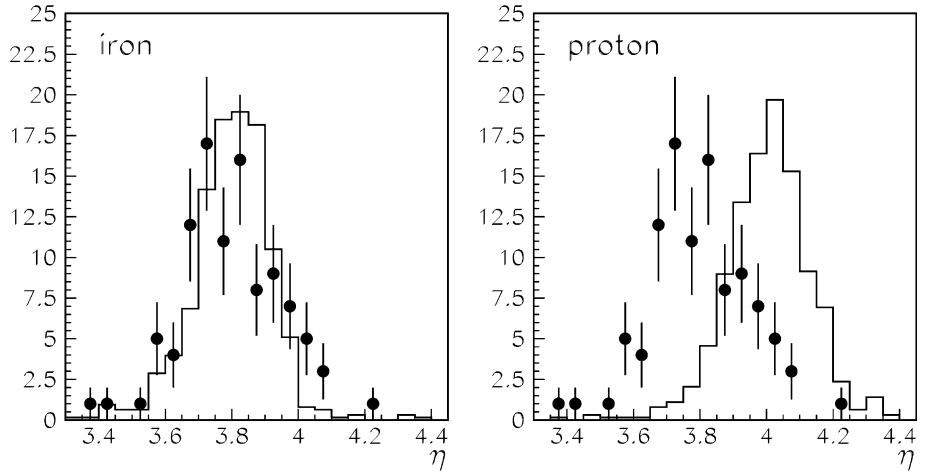

Fig. 6. The measured distributions of η (data points) with histograms from Monte Carlo calculations of pure iron (left) and pure proton (right) with $1.0 < \sec\theta < 1.1$, using QGSJET98.

In Fig. 6 we compare the Monte Carlo results with the Volcano Ranch data points for near-vertical showers. As can be seen, the tail at large η in the comparison with iron indicates that a lighter component is required to fit the experimental data. The best fit gives a mixture with $(89 \pm 5)\%$ of iron, with a corresponding percentage of protons, and this distribution of η is shown in Fig. 7.

The raw data for each of the events included in Figs. 6 and 7 are not available to us and therefore it has not been possible to assign energies to individual events. What is recorded is that the median energy was 10^{18} eV and that the shower sizes are between 4×10^7 and 6×10^9. This corresponds to an energy range between 10^{17} and 10^{19} eV. To reproduce the data set, a differential energy spectrum of slope -3.5 was chosen for the primary energy spectrum. Simulations show that the whole area of the array was active above 10^{18} eV. Using this spectrum and the condition that the median energy be 10^{18} eV, the calculated threshold energy is approximately $10^{17.7}$ eV.

Below 10^{18} eV the energy distribution of the data set was smoothed (always under the condition of the median energy being 10^{18} eV) assuming that the effective area of the detector increases with energy from the threshold up to 10^{18} eV. The conclusions about mass composition that we presently draw are significantly constrained by uncertainties in the details of the energy distribution of events recorded at Volcano Ranch. The systematic error arising from our lack of knowledge of the energy distribution of the events has been estimated by repeating the fitting procedure with different energy spectra. From this analysis we estimate this error to be 12%.

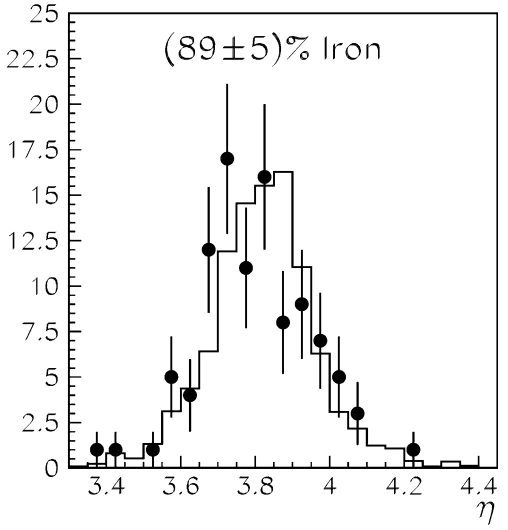

Fig. 7. Composition fit from η distribution for the first bin in $1.0 < \sec\theta < 1.1$, using QGSJET98. The points are the VR data and the solid line corresponds to the result of the fit.

An additional source of systematic error is related to uncertainties in the hadronic interaction model; following the discussion in [1], which relates to the use of QGSJET98 rather than QGSJET01, the systematic shift in the fraction of iron is 14%. Showers that are calculated using QGSJET01 are found to develop higher in the atmosphere so that the fraction of Fe estimated is reduced from $(89 \pm 5)\%$ to $(75 \pm 5)\%$.

6. Comparison with other data

In Fig. 8, we show the results from various reports of the Fe fraction as a function of energy, as inferred from a variety of techniques. The Volcano Ranch data have been represented by a single point (with an error bar) at the median energy of the events; this energy is based on Linsley's estimate and is believed to be reliable. Horizontal lines have been drawn to indicate the range of energies in the data, as described above. The error at the lower bound may be similar to the error shown at the median (as it is close in energy), but the error at the upper end must surely be greater as the number of events must have been small. There is, however, no reliable way of computing errors at either end of the range.

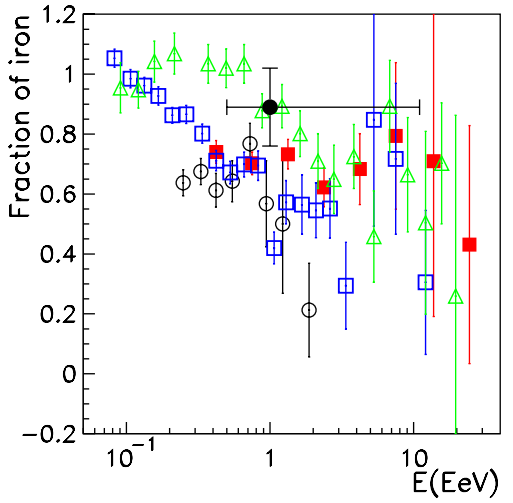

Fig. 8. Fe fraction from various experiments: Fly's Eye (△), AGASA A100 (■), AGASA A1 (□) using SIBYLL1.5 ([6] and references therein) and Haverah Park [1], using QGSJET98 (○). The mass composition determined in this paper from Volcano Ranch data, using QGSJET98 (●), is shown, together with an estimate of the error and energy range.

The data from Volcano Ranch and from Haverah Park [1] are not in good agreement despite the facts that a similar quantity, the lateral distribution function of the showers, has been measured at each array and that the same model (QGSJET98) was used to interpret the data (although with different propagation codes, AIRES and CORSIKA, respectively). We cannot explain this difference.

In Fig. 8 we also show data from the Akeno/AGASA and the Fly's Eye experiments. The Akeno/AGASA groups measured the muon densities in showers, normalized at 600 m. The energy thresholds for Akeno and AGASA were 1 and 0.5 GeV, respectively. The Fly's Eye data are deduced from measurements of the depth of shower maximum. In an effort to reconcile differing claims made by the two groups for the trend of mass composition with energy, Dawson et al. [6] reassessed the situation using a single model, SIBYLL1.5, on both data sets. SIBYLL1.5 was an early version of the SIBYLL family that evolved to SIBYLL1.6, 1.7 and 2.1. It is the estimates of the Fe fractions from [6] that are shown in Fig. 8. However, the predictions of the muon density and of the depth of shower maximum made with the version of SIBYLL used in [6] differ significantly from those that would be derived using QGSJET98 or QGSJET01 (or with the later SIBYLL version, 2.1). We now discuss this point in some detail drawing on the extremely useful set of comparisons of the predictions from SIBYLL1.7 and 2.1 with those from QGSJET98 which has been given in [28]. We understand that SIBYLL1.6 and SIBYLL1.7 differed only in that the neutral pions were allowed to interact in the latter model and it is not believed that this will make a serious difference to the predictions at energies below 10^{19} eV [29]. Therefore, in what follows we regard the SIBYLL1.7 and QGSJET98 differences as being identical to those that exist between SIBYLL1.6 (or 1.5) and QGSJET98, for which no similar comparisons are available. It is convenient to make comparisons between model predictions at 10^{18} eV. More detailed comparisons, over a range of energies,

would require a more extensive knowledge of features of the Fly's Eye and Akeno/AGASA systems than we possess.

Turning first to the data from the depth of maximum [30], we note that at 10^{18} eV the measured value of $X_{\max}$ is $\approx$675 g cm^{-2}, with an error that is less than the size of the data point ($\leqslant$10 g cm^{-2}). The predictions for proton primaries made with SIBYLL1.7 and QGSJET98 are 760 and 730 g cm^{-2}, respectively [28]. Thus, a mass composition a little less dominated by iron is favored compared with the $\approx$90% estimated in [6]. The choice of SIBYLL2.1 would alter this argument rather little, as the predicted depth [28] at 10^{18} eV is 740 g cm^{-2}. Although it is not possible to provide a direct comparison of our result obtained over an energy range with median energy of 10^{18} eV, it could be in agreement with that obtained by Fly's Eye experiment at 10^{18} eV. Further study of this matter could be made, but the data from Fly's Eye should soon be superseded by definitive data from the HiRes stereo system.

A qualitative statement about the shift expected in the Fe fraction, as estimated from the measurement of muon densities at 600 m, can be made using the information in [28]. Although the calculations do not exactly match the energies of the Akeno/AGASA measurements ($\geqslant$0.3 GeV was computed and $\geqslant$0.5 GeV was measured), the ratios between the predictions of different models are not strongly dependent upon energy threshold. What is of importance is the ratio of the number of muons predicted for SIBYLL1.7, SIBYLL2.1 and QGSJET98. At 10^{18} eV these numbers are in the ratios 1:1.17:1.45.

The difference in muon number between SIBYLL1.7 and QGSJET98 is comparable to that expected between proton and Fe primaries ($\approx$50%, but also model dependent). It is clear that the more recent models, if applied to the Akeno/AGASA data, after the manner of the analysis of [6], would lead to a significant reduction in the predicted fraction of Fe nuclei. To pursue this further would require knowledge of the predicted densities at 600 m, information that is presently lacking. We note that the shift in the Fe fraction from the muon data is probably substantially larger than it is when using the data on $X_{\max}$.

We have not shown the data reported from the HiRes/MIA experiment in which muons and $X_{\max}$ were observed simultaneously [7]. As with Akeno/AGASA, the muon density at 600 m was determined. The problem we have is that while the papers describe the data as being consistent with a mass composition that becomes lighter with energy, this appears, on close scrutiny of Figs. 1 and 2 of [7], to be true only for the $X_{\max}$ data. The muon data, which are compared with predictions of QGSJET98, appear to be consistent with a constant and heavy mass from 5×10^{16} to beyond 10^{18} eV.

It would be interesting to establish that the same model gives different predictions for the mass variation with energy for different measured quantities: this might lead to further understanding of the models or the systematic errors in different measurements, but it is not a matter on which we can speculate here. [1]

The above discussion demonstrates the difficulties that one is faced with when trying to compare data. The measurements from different experiments are often not analyzed contemporaneously and the shifts in the inferences can be substantial when different models are used. In this context, we believe that the present analysis of the Volcano Ranch data is useful but it is clear that other measurements are needed before final conclusions can be drawn. Such conclusions will, however, be subject to revision as models evolve. For example, in [1], the average fraction of Fe inferred using QGSJET98 was 0.66; with QGSJET01 the fraction was 0.52. Therefore we expect a similar shift for the Volcano Ranch data.

7. Conclusions

Measurements of the steepness of the lateral distribution η were made at Volcano Ranch on a shower-to-shower basis for fixed bins of zenith angle. We have compared the measured

[1] While revising this paper we received a preprint of a review paper of Engel and Klages in which a similar conclusion is reached [31].

distribution of η to our Monte Carlo results for proton and iron primaries using QGSJET98 including the scintillator response of the detectors in the Volcano Ranch array. Our ability to reproduce Volcano Ranch lateral distribution measurements gives us confidence that our analysis procedure is sound.

The cosmic ray mass composition, deduced from Volcano Ranch data, is compatible with mean fraction $(89 \pm 5(\text{stat}) \pm 12(\text{sys}))\%$ of iron in a bi-modal proton and iron mix, in the whole energy range $10^{17.7}$ eV to 10^{19} eV, with mean energy 10^{18} eV. Following the discussion in [1], we estimate that this fraction would be reduced to 75%, with the same QGSJET01 model adopted.

The inconsistencies that exist between several experiments which spanning energy ranges using different techniques, is enhanced, as different hadronic models are used for the interpretation of the raw data. While Haverah Park, Volcano Ranch and Akeno-AGASA infer $X_{\max}$, and hence the overall composition, from properties of secondary particle distributions at ground, Fly's Eye and HiRes experiments observe an image of the longitudinal shower profile and measure $X_{\max}$ directly. Nonetheless the estimates can be biased due to poor knowledge of atmospheric properties as recent studies of atmospheric profiles have suggested [27].

In this context, we believe that the present analysis of the Volcano Ranch paper is useful, but other existing data are desirable, preferably with the same hadronic models used for the interpretation. The differences between measurements of mass composition need to be addressed further if more solid conclusions on the origin, acceleration or propagation of cosmic rays are to be reached. The rate of change of the average mass with energy is still under debate.

Acknowledgements

We warmly thank the late John Linsley for discussions regarding his data during the 27th ICRC in Hamburg, and for his permission to proceed with an analysis along the lines described above. However, the interpretation given is that of the authors alone, as it was not possible to discuss the outcome of the work with him before his death.

We are grateful for the comments of a referee, who has helped us to clarify some aspects of the paper, and to Todor Stanev, Jim Matthews and Bruce Dawson for helpful explanations about the SIBYLL series of models.

Work at Universidad de La Plata is supported by ANPCyT (Argentina), at Northeastern University by the US National Science Foundation and at the University of Leeds by PPARC, UK (PPA/Y/S/1999/00276). TPM gratefully acknowledges the support of the American Astronomical Society in the form of a travel grant to attend the 28th ICRC in Tsukuba, Japan, where a version of this work was presented. MTD thanks the John Simon Guggenheim Foundation for a fellowship.

References

[1] M. Ave et al., Astropart. Phys. 19 (2003) 61.
[2] D.J. Bird et al., Phys. Rev. Lett. 71 (1993) 3401.
[3] D.J. Bird et al., in: Proceedings of the 23th ICRC, Calgary, vol. 2, 1993, p. 38.
[4] N. Hayashida et al., J. Phys. G 21 (1995) 1101;
S. Yoshida et al., Astropart. Phys. 3 (1995) 105.
[5] K. Shinozaki et al. (AGASA Collaboration), in: Proceedings of the 28th ICRC, Tsukuba, 2003, p. 401.
[6] B.R. Dawson, R. Meyhandan, K.M. Simpson, Astropart. Phys. 9 (1999) 331.
[7] T. Abu-Zayyad et al. (HiRes/MIA Collaboration), Phys. Rev. Lett. 84 (2000) 4276;
T. Abu-Zayyad et al. (HiRes/MIA Collaboration), Astrophys. J. 557 (2001) 686.
[8] G. Archbold et al. (HiRes Collaboration), in: Proceedings of the 28th ICRC, Tsukuba, 2003, p. 3405.
[9] B.N. Afanasiev et al., in: Proceedings of the Tokyo Workshop on Techniques for the Study of the Extremely High Energy Cosmic Rays, 1993, p. 35;
M. Nagano (Ed.), Institute for Cosmic Ray Research, University of Tokyo.
[10] S. Sciutto, in: Proceedings of the 27th ICRC, Hamburg, 2001.
[11] N.N. Kalmykov, S.S. Ostapchenko, Yad. Fiz. 56 (1993) 105;
N.N. Kalmykov, S.S. Ostapchenko, Phys. Atom. Nucl. 56 (1993) 346;
N.N. Kalmykov, S.S. Ostapchenko, Bull. Russ. Acad. Sci. (Phys.) 58 (1994) 1966;
N.N. Kalmykov, S.S. Ostapchenko, A.I. Pavlov, Nucl. Phys. 52B (1997) 17.

[12] R. Engel, T.K. Gaisser, T. Stanev, in: Proceedings of the 26th ICRC, Salt Lake City, vol. 1, 1999, p. 415.
[13] D. Heck (Kascade Collaboration), in: Proceedings of the 27th ICRC, Hamburg, 2001.
[14] M. Nagano et al., Astropart. Phys. 13 (2000) 277.
[15] S. Agostinelli et al. (Geant4 Collaboration), Nucl. Instrum. Methods A 506 (2003) 250. Available from <http://geant4.web.cern.ch/geant4>.
[16] J. Linsley, L. Scarsi, B. Rossi, Phys. Rev. Lett. 6 (1961) 485.
[17] A.M. Hillas, Nucl. Phys. B (Proc. Suppl.) 52B (1993) 29;
A.M. Hillas, in: Proceedings of the 19th ICRC, La Jolla, vol. 1, 1985, p. 155.
[18] A.M. Hillas, in: J. Linsley, A.M. Hillas (Eds.), Proceedings of the Paris Workshop on Cascade Simulations, 1981, p. 39.
[19] J. Linsley, Phys. Rev. Lett. 10 (1963) 146.
[20] J. Linsley, in: Proceedings of the 15th ICRC, Plovdiv, vol. 12, 1977, p. 56.
[21] J. Linsley, in: Proceedings of the 15th ICRC, Plovdiv, vol. 12, 1977, p. 62.
[22] J. Linsley, in: Proceedings of the 15th ICRC, Plovdiv, vol. 12, 1977, p. 89.
[23] T. Kutter, Auger Technical Note GAP-98-048. Available from <http://www.auger.org>.
[24] J. Linsley, in: Proceedings of the 13th ICRC, Denver, 1973, p. 3212.
[25] A.M. Hillas, Acta Phys. Acad. Sci. Hung 29 (Suppl. 3) (1970) 355;
A.M. Hillas et al., in: Proceedings of the 12th ICRC, Hobart, vol. 3, 1971, p. 1001.
[26] M.T. Dova et al., Nucl. Phys. B (Proc. Suppl.) 122 (2003) 235.
[27] B. Keilhauer et al., in: Proceedings of the 28th ICRC, Tsukuba, 2003, p. 879.
[28] J. Alvarez-Muñiz et al., Phys. Rev. D 66 (2002) 033011.
[29] T. Stanev, private communication, February 2004.
[30] T.K. Gaisser et al., Phys. Rev. D 47 (1993) 1919.
[31] R. Engel, H. Klages, Comptes Rendus Physique 5 (4) (2004) 505–518.